Degradation Characteristics of Porous Fe-Mn-C Alloys Obtained by Sintering-Dissolution Process (SDP) for Metallic Bone Scaffold

(Pencirian Degradasi Aloi Poros Fe-Mn-C Diperoleh daripada Proses Pembubaran Sinter (SDP) untuk Perancah Tulang Metalik)

YUDHA PRATESA, ALMIRA LARASATI, SRI HARJANTO*, BAMBANG SUHARNO & MYRNA ARIATI

ABSTRACT

Porous degradable metal is a promising material for hard-tissue scaffold application. It offers better mechanical properties than polymer and easier cell proliferation. However, the corrosion process in the porous metallic implant usually causes toxicity on patient. Therefore, corrosion process is the key for the development of the alloy. The previous study has successfully formed a porous Iron-35%Manganese-1%Carbon (Fe-35Mn-1C) alloy using Potassium carbonate (K_2CO_3) as foaming agent with powder metallurgy process. This study focused on the degradation behavior and phase analysis of Fe-Mn-C product by polarization test in ringer solution, Atomic Absorption Spectrometry (AAS), X-Ray Diffraction, and Energy Dispersive Spectroscopy. This process resulted in nonmagnetic Austenitic phase that is beneficial for MRI application. The result showed that Fe-Mn-C alloy with foaming structure is suitable for degradable biomaterials. The density of the product is 3.2 gr/cm³, which is only half of the bulk material. The degradation rate of the metals also increases to 6 mm/year, but the maximum ion released is still under the limit in terms of toxicity against human.

Keywords: *Degradable biomaterials; Fe-35Mn-1C; powder metallurgy; sinter dissolution process (SDP)*

ABSTRAK

Logam degradasi berliang adalah bahan yang berpotensi untuk dibangunkan sebagai perancah tisu keras. Ia menawarkan sifat mekanik yang lebih baik daripada polimer. Struktur poros bermanfaat untuk percambahan sel yang tinggi dalam implan. Walau bagaimanapun, proses kakisan dalam biomas bahan metalik menyebabkan ketoksikan pada pesakit. Oleh itu, proses kakisan adalah kunci kepada perkembangan aloi. Kajian terdahulu telah berjaya membentuk aloi besi-35% Manganese-1% Karbon (Fe-35Mn-1C) menggunakan potasium karbonat (K_2CO_3) sebagai agen berbuih dengan proses metalurgi serbuk. Kajian ini menumpukan kepada tingkah laku perosak dan analisis fasa produk Fe-Mn-C melalui ujian Polarisasi dalam penyelesaian dering, Spektrometri Penyerapan Atom (AAS), Difraksi X-Ray dan Spektroskopi Penyebaran Tenaga. Hasilnya menunjukkan bahawa aloi Fe-Mn-C dengan struktur buih sesuai untuk degradasi biobahan. Ketumpatan produk adalah 3.2 gr/cm³, yang hanya separuh daripada bahan pukal, kadar degradasi logam juga meningkat kepada 6 mm/tahun tetapi keluaran ion maksimum di bawah paras ketoksikan pada manusia. Ia membentuk fasa Austenitic yang merupakan fasa nonmagnetik dan selamat untuk aplikasi MRI.

Kata kunci: *Degradasi biobahan; Fe-35Mn-1C; metalurgi serbuk; proses pembubaran sinter (SDP)*

INTRODUCTION

The development of the degradable implant, that shifting to the degradable porous biomaterial, offers better cell attachment for bone scaffold applications. The main focus of the development of scaffold material is the morphology and the amount of porosity. The morphology of porosity affects the mechanical properties of the implant. Irregular porosity is widely known to be able to act as crack initiation (Murphy et al. 2010). High porosity can reduce the compressive strength of materials and increase the rate of degradation (Pratesa et al. 2018). Therefore, the porosity can solve low degradation rate problem of Iron-based biomaterials. In the future, one can easily adjust the lifespan of a scaffold by engineering the number of porosities in implant materials.

Foamed structured Fe alloy was successfully fabricated through a powder metallurgy process. The types of space holder and filler material have important roles in the porosity design. Ammonium bicarbonate (Čapek et al. 2015; Zhang & Cao 2015), potassium carbonate (Pratesa et al. 2018), and carbamide (Pratesa et al. 2018) have been proposed as filler material in metal foam fabrication. Each of the space holder agents has different porosity morphology and porosity numbers, as shown in Table 1.

Nowadays, Fe-Mn-C alloy attracts many researchers to study it as a degradable implant. This alloy is a non-magnetic material, which is suitable for the Magnetic Resonance Imaging (MRI) examination. Non-magnetic behavior makes the implant easier to be distinguished in the MRI images. Iron and Manganese also have a high

TABLE 1. Study of filler materials for Fe-Mn foam structured alloy

Filler Materials	Materials	Morphology	% Porosity	Author
Carbamide	Fe-35Mn-C	Spherical	52	Pratesa et al. (2018)
Potassium carbonate	Fe-35Mn-C	Irregular	60	Pratesa et al. (2018)
Ammonium bicarbonate	Fe 35Mn	Irregular	32-82	Čapek et al. 2015)
Ammonium bicarbonate	Fe 35Mn	Irregular	25-31	Zhang et al. (2015)
Ammonium bicarbonate	Fe30Mn	Irregular	60%	Huang et al. (2019)
NaCl	Fe-Mn-Si-Pd	Irregular	26-63	Feng et al. (2017)

tolerance limit in human's body, hence this alloy does not have toxicity issue. Feng et al. (2017) show that Fe-Mn-Si-Pd foam alloy, produced using 10 % NaCl addition, has good cell viability.

Our previous study has successfully formed porous Fe-35Mn-1C material using potassium carbonate (K_2CO_3) as the foaming agent with the powder metallurgy process. Potassium carbonate was selected as a foaming agent due to its ability to decompose in the sintering temperature of Fe-35Mn-1C. Potassium carbonate also increased porosity and corrosion rate. It produces Kohenite phase (iron carbide) as the by-product (Harjanto et al. 2012). This study uses various potassium carbonates composition to get a better understanding of porosity effect in corrosion rate of the alloy and also to study the ion release behavior from each element. The ion release behavior can be used to predict the toxicity level based on the maximum uptake level of element in the human body.

Various studies have been carried out to find suitable fillers for the Sintering Dissolution Process (SDP) and to improve corrosion and mechanical properties of the alloy. A number of studies utilize porosity to regulate the lifespan of an implant. Therefore, an in-depth study is needed to determine the relationship between microstructure and corrosion rate of porous material in order to obtain the desired corrosion rate. Moreover, a study about the number of ions released into solution is also an exciting area, since it is related to the toxicity of an implant (Huang et al. 2019). Therefore, this study aims to understand the correlation between the number of porosity, microstructure, and corrosion behavior of the alloy, produced by utilization of potassium carbonate as foaming agent. This correlation is essential data to manipulate the degradation rate of the alloy.

MATERIALS AND METHODS

MATERIAL

The alloys were prepared using a powder metallurgy process. Potassium carbonate (K_2CO_3) was added as the foaming agent. This study used 5, 10, and 15 wt. %, respectively, of K_2CO_3. These variables aim to produce different porosity content in the material. Green product was made by high purity iron powder (Merck, 99 %), ferromanganese powder (76 % Mn, 1 % C, and 1.47 % Si),

and carbon (fine powder, 99 %). All of the powders were mixed to achieve the target composition of Fe-35Mn-1C. After the mixing process, potassium carbonate (K_2CO_3) was added to the powders. Then, it was milled using mortar for 10 min to distribute the potassium carbonate. The size of iron powder is 74 μm, while ferromanganese powder and potassium carbonate were 88 μm and 125 μm, respectively. The sample was pressed in cylinder dies (10 mm diameter and 10 mm height) using uniaxial force. It was pressed at 36 kg/cm2 for 15 min.

Green product was sintered with a double step sintering process in the nitrogen gas atmosphere to prevent oxidation of the powder during the process. The first step (3 h, 850 °C) was used for thermal decomposition from K_2CO_3, and the second step, sintering (1.5 h, 1100 °C), was performed for austenite formation and further densification.

METHODS

Physical characterization was conducted for the number and size of porosity and density of the sintered product. Porosity and density were measured using Archimedes method based on ASTM A378-88. It compared the mass of the product in the air and fluid. This test used oil for the testing fluid. It was chosen to minimize corrosion and K_2CO_3 dissolution that could happen during the test. Field Emission-Scanning Electron Microscope (FE-SEM) was used to measure the porosity size. It was also used to characterize the morphology of the sintered product. Density calculation was conducted with the following equation:

$$\rho_{archimedes} = \frac{M_{air}}{M_{oil}} x \rho_{oil}$$

(1)

$$\rho_{teoritical} = \left(\rho_{Fe} x \%_{wt\ Fe} \right) + \left(\rho_{FeMn} x \%_{wt\ FeMn} \right)$$
$$+ \left(\rho_{C} x \%_{wt\ C} \right) + \left(\rho_{K2CO3} x \%_{wt\ K2CO3} \right)$$

(2)

Degradation behaviors were analyzed with potentiodynamic polarization corresponding to ASTM G5 and Atomic Absorption Spectrometry (AAS). Both corrosion characterization methods used ringer lactate

solution as Simulated Body Fluid (SBF) at room temperature (28 °C). Ringer lactate has been known for isotonic with blood fluid. Hence, it could be a good representative of blood electrolytes. Composition of the ringer lactate is NaCl (6.0 gr/L), KCl (0.30 gr/L), $CaCl_2$ (0.20 gr/L), $C_3H_5NaO_3$ (3.10 gr/L). This polarization test used a Standard Calomel Electrode (SCE) as the reference electrode and carbon graphite as the counter electrode with a scan rate of 0.1 v/s. The samples were immersed in the test solution for 10 min before the testing to stabilize the sample. The current density was analyzed using Tafel plot methods. The current density was used for corrosion rate calculation using (3):

$$Corrosion\ rate = \frac{KIEw}{\rho} \tag{3}$$

where K is the Constant = 3.27×10^{-3} mm g/μA.cm.y; I -Current density from the Tafel plot (A/mm^2); Ew is the equivalent weight; and ρ is the density (g/mm^3).

Degradation behavior of the element was analyzed using Atomic Absorption Spectrometry. It used supernatant immersion fluid from the immersion test. The duration of the immersion test was 24, 72, and 168 h. The data were used to examine the ion release of the element per day.

Phase analysis was conducted using Energy Dispersive Spectroscopy (EDS), Field Emission-Scanning Electron Microscope (FE-SEM), and X-ray diffraction (XRD). Backscattered imaging (BSE) was used to give a contrast between the alloying elements. The microstructure of the sintered product was analyzed by metallographic test with Nital 2 % as the etching solution.

RESULTS AND DISCUSSION

PHYSICAL CHARACTERIZATION

The porosity increased when more K_2CO_3 was added to Fe-35Mn-1C alloy. The highest porosity number is 60 %, which resulted from 15 % K_2CO_3. As a result of porosity formation, volume expansion directly happened after the sintering process. CO_2 gas formation that was generated from K_2CO_3 decomposition, caused volume expansion (Pratesa et al. 2018). The final product had isolated and irregular porosity, as shown in Figure 1.

Potassium carbonate decomposition is described in (4). Lehman et al. (1998) reported that potassium carbonate decomposed near their melting point in the CO_2/N_2 atmosphere. The vapor pressure of K_2CO_3 increased at the temperature above 900 °C, followed by the weight loss (Murphy et al. 2010). The vapor pressure of K_2CO_3 could reach 1000 Pa at temperature 1100 °C, which made decomposition of K_2CO_3 is highly possible in this study.

$$K_2CO_3 \rightarrow K_2O + CO_2 \tag{4}$$

As a result of decomposition, porosities were formed and density was reduced. This resulted in improving strength to weight ratio of iron based biomaterial to become near the bone value. Table 2 shows a comparison of several implant materials density and bone.

Foam structured material has a similar density as natural bone. The apparent density with K_2CO_3 agent is only a half than planetary ball mill process from 7.2 g/cm^3 to 3.5 g/cm^3 (Harjanto et al. 2012).
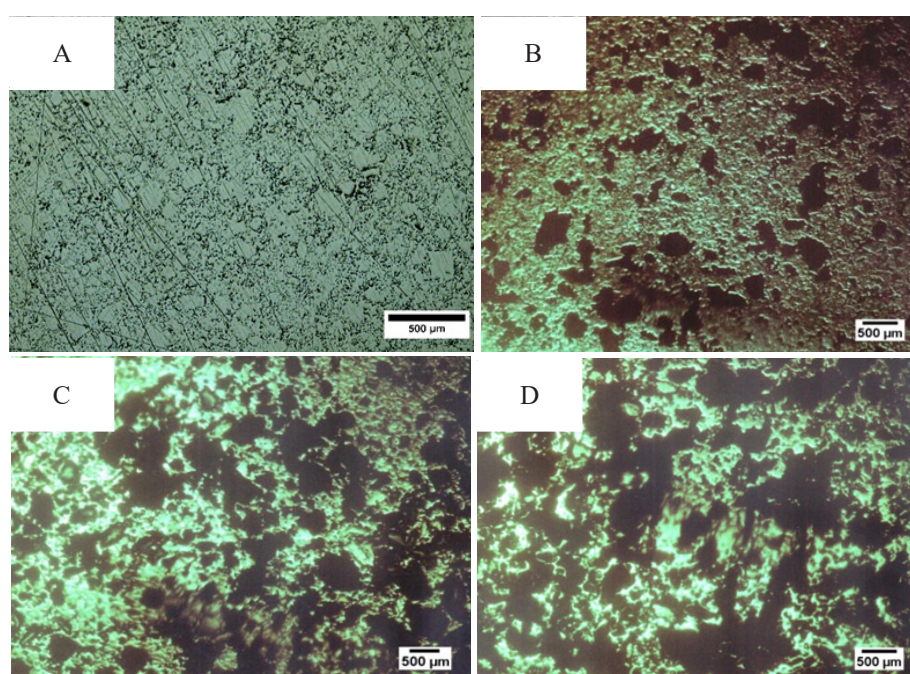

FIGURE 1. Morphology of materials Fe-35Mn-1C with variation of K_2CO_3 composition of (A) 0 % , (B) 5 %, (C) 10 % and (D) 15 %

TABLE 2. Comparison of this study and other materials implant candidate

Materials	Density (g/cm³)	References
Bone	1.15	Witte et al. (2008)
Magnesium	1.74	Chakraborty et al. (2019)
Magnesium Foam	0.572	Osorio-Hernández et al. (2014)
Fe-Mn-Si-Pd(10 wt. % NaCl)	5.3	Feng et al. (2017)
0% K_2CO_3	7.30	Pratesa et al. (2018)
5% K_2CO_3	4.10	This study
10% K_2CO_3	3.62	This study
15% K_2CO_3	3.49	This study

As reported in the previous study, porous metallic material is a good candidate for bone implants as larger porosity is needed for lamellar bone formation and osteon growth (Shah et al. 2019). The optimal size of porosity for cell adhesion is known to be around 300 μm (Murphy et al. 2010). This study produced a variety of sizes from 200 to 600 μm, which is around the number stated by Murphy et al. (2010). However, some of the porosities are four times larger compared with potassium carbonate powder size. These large porosities showed that agglomeration happened when higher amount potassium carbonate was added into the powder mixtures.

PHASE ANALYSIS

The alloys have non-magnetic phase (Austenite) as the majority phase, due to manganese diffusion into the Fe matrix. Figure 2 shows the X-ray Diffraction (XRD) analysis of non-foam Fe-35Mn-1C alloy and foam structured Fe-35Mn-1C. Benz et al. (1973) show that Fe-Mn-C at 1100 C should contain Austenite only. However, this study found a different result where the cohenite (Fe_3C) phase is found, which shows higher amount of carbon atoms is successfully diffused in the iron matrix. Overall, the phase consisted of austenite (γ), manganese oxide (MnO), and cohenite ($(Fe,Mn)_3C$) in the final product (Pratesa et al. 2018). The phase was independent of the number of filler material added to the alloy. Cohenite is assembled by the diffusion of carbon from CO_2 gas as the result of potassium carbonate decomposition.

Figure 3 shows the microstructure of the porous Fe-Mn-C alloy etched by Nital. The microstructure shows austenite phase (white), porosity (black), and cohenite (lamellar). The result confirmed the XRD analysis result from each of the phases. The cohenite phase significantly increased in the higher number of K_2CO_3. With 15 % of potassium carbonate addition, the cohenite phase has a lath lamella. However, with 10 % potassium carbonate addition, the lamella is fine and located in the middle of the grain. Overall, the grain was surrounded by a thin white layer. This layer is undiffused manganese that remains in the surface of the iron particle. The undiffused manganese condensed in the surface of the particle and created MnO. The confirmation of MnO phase were then shown in the EDS analysis.

Characterization of porosity was done using the EDS examination, and the result is shown in Table 3. The porosities were surrounded by manganese oxide. EDS shows that the brown area is rich with manganese. It shows that manganese is always found at the surface of the grain. It indicates the existence of manganese alloyed iron powder with solid-gas phenomenon. Manganese has low vapor pressure, hence, it can sublimate at a temperature below the melting point (Šalak & Selecká 2012). The manganese vapor will diffuse into the iron matrix, and the remnant vapor sticks in the grain boundary area after the cooling process. Then, manganese will be transformed into MnO in the final condition. Carbon increased from 1 wt. % to 6-7 wt. % is caused by the carburization process. Based on Bouduard diagram, CO_2 as a product of potassium carbonate decomposition could react with carbon (graphite) to make carbon monoxide (CO) with a reaction.

$$C + CO_2 \rightarrow 2CO \qquad (5)$$

A high ratio of CO/CO_2 created a carburization process and added more carbon that was diffused into the iron. In this alloy system, K_2CO_3 decomposition generated more CO_2, which, based on reaction 5, the CO_2 reacted with graphite to produce more CO.

CORROSION BEHAVIOUR

The potentiodynamic polarization result is shown in Figure 4. The corrosion current densities increase from 60 to 231 μA/cm³, which is an indication of corrosion rate enhancement. This result is caused by the higher complexity in the material phase. K_2CO_3 makes the number of porosities, MnO_2, and cohenite phase increased significantly, as shown in the XRD result. Moreover, Figure 4 shows a shifting of the corrosion potential (E_{corr}) into the lower value. Corrosion potential shifting is usually associated with the surface activity of the materials. Macro porosity increases the corrosion potential of the alloy to the higher value and decreases slightly as the porosity number also increases. The formation of MnO and cohenite could contribute to the potential corrosion declination above 10 % porosity.
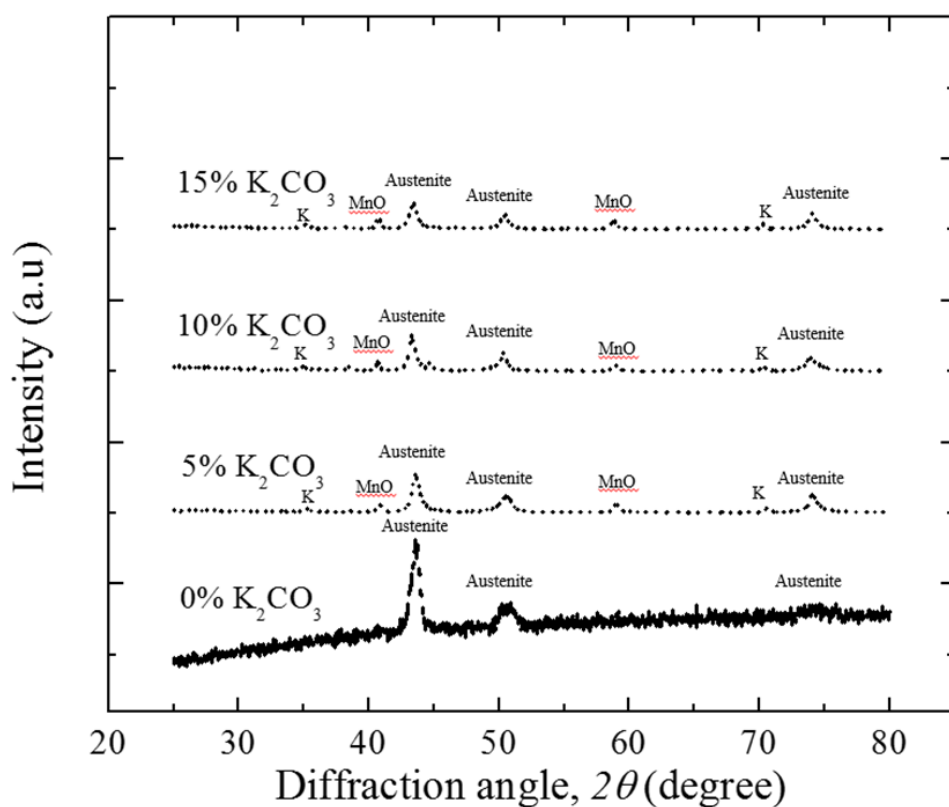
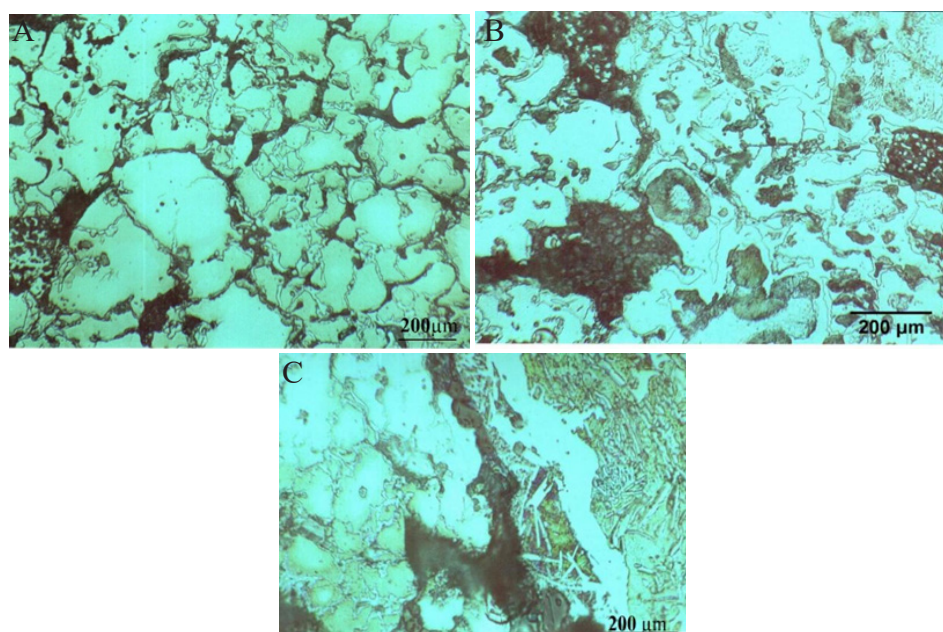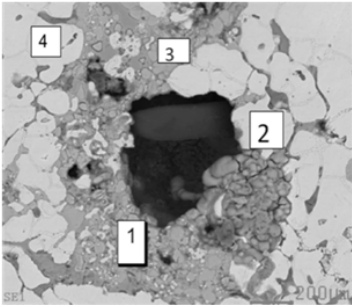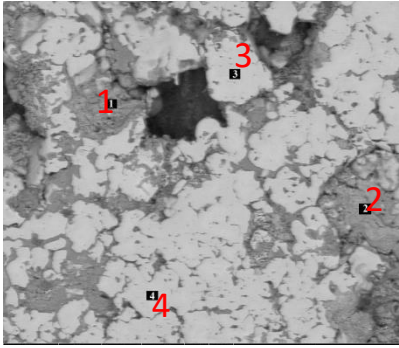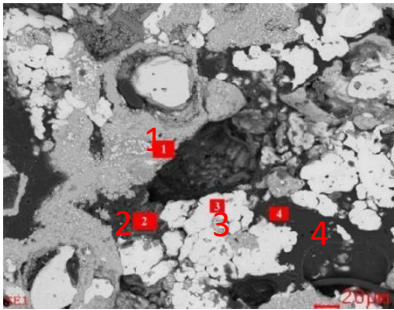FIGURE 2. Effect of potassium carbonate in Fe-Mn-C alloy formed a Cohenite phase

FIGURE 3. Microstructure of sintered product showed austenite (white), porous (black) and cohenite (lamellar) from (a) 5 %, (b) 10 % and (c) 15 % of K_2CO_3

Figure 5(A) shows the polarization curve of each alloy shifted to the higher number of current density. In detail, the anodic curve did not shift significantly compared to the cathodic curve. The cathodic curve shiftings indicated that the corrosion is controlled by the cathodic reaction.

The cathodic reaction in the neutral-NaCl solution is dominantly caused by O_2 reduction. This oxygen reduction takes place in the cathodic phase, such as MnO.

Based on the corrosion potential, MnO will act as cathodic and austenite as an anodic site. Details of the

TABLE 3. EDS spot analysis for each phase

Location	EDS result

No	Fe(%)	Mn(%)	C(%)	Si(%)	O(%)
1	-	71,8	4,5	2,1	21,6
2	74,9	19,9	5,1	-	-
3	-	64,1	6,1	2,7	26,6
4	82,9	11,1	5,9	-	-

No	Fe(%)	Mn(%)	C(%)	Si(%)	O(%)
1	-	49,7	7,9	4,1	36,85
2	-	65,6	6,9	5,6	21,9
3	77,9	16,2	5,9	-	-
4	80,9	12,9	6,2	-	-

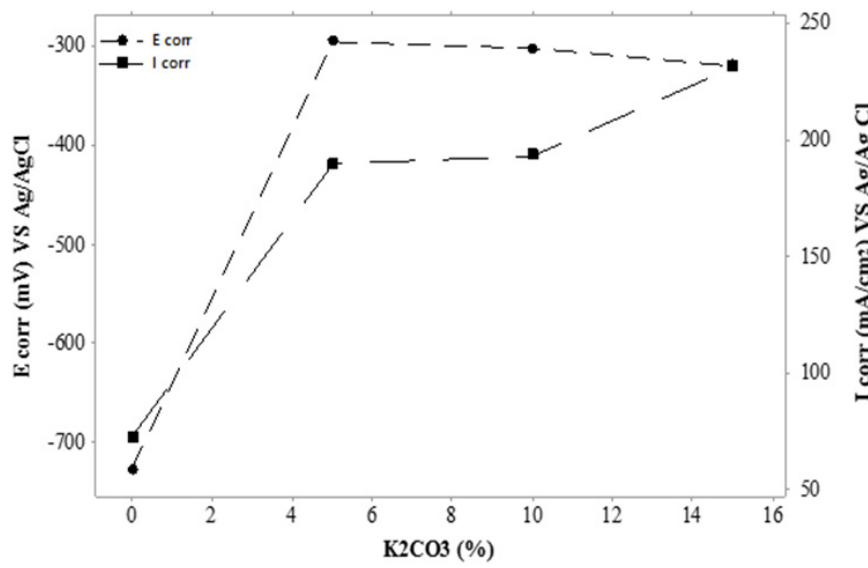| No	Fe(%)	Mn(%)	C(%)	Si(%)	O(%)
1	-	59,4	7,6	7,4	25,5
2	1,5	5,3	59,7	-	31,3
3	74,9	11,8	7,2	-	6,0
4	-	-	76,3	-	23,7

FIGURE 4. Corrosion potential and current density of Fe-35Mn-C foam structured materials

phase's role in the alloy are elaborated further in the AAS result. Besides the effect of MnO, the shifting of the curves can be correlated with the surface condition of the metals. A higher porosity means a higher surface area for the cathodic reaction. Therefore, it was possible that the porosity contributes to the corrosion phenomenon in a metal foam.
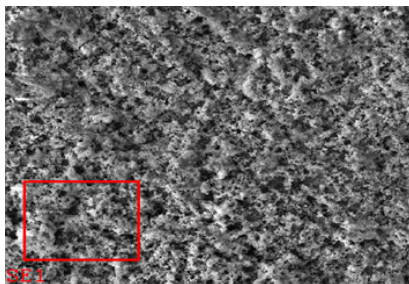
Based on EDS and Polarization analysis, each of porosities is surrounded by manganese oxide due to the small proportion of manganese that did not diffuse during the sintering process making a bond with oxygen and forming MnO at the porosity. The MnO affected the corrosion rate of the alloy due to the different potential between manganese oxide and the austenite phase. This condition makes a micro galvanic is possible at the Fe-Mn-C porous material (Figure 5(B)).

The ion release test was done using atomic absorption spectroscopy (AAS). This result was taken from the supernatant liquid in order to measure a number of freed ion due to the corrosion process. The result shows iron and manganese ion decreased after 72 h due to scale formation, as illustrated in Table 4. The scale prevented the solution from direct contact with surface material and caused the corrosion rate to decline after 72 h.

Figure 6 shows the Fe ion released into the solution is higher than manganese. This condition supports our theory about the galvanic reaction between the phases. It shows the austenite (Fe) area as an anode, while MnO as a cathode. During the 24 h immersion, the iron release was high, and the rate declined after 24 h. On the other hand, manganese ion was still very low after 24 h immersion and increased in 48 h. It is solid evidence that galvanic reaction happened in the alloy which caused the selective leaching on the austenite phase and was followed by MnO later. Five percent K_2CO_3 has the highest ion release than the others. However, the result was the opposite of polarization, which shows corrosion rate was affected by the number of porosities. This phenomenon could be elucidated by film formation. AAS was taken from the supernatant fluids, which described the number of ions released into the solution, while most of the ion was highly possible to transform into an oxide layer. In the polarization test, the effect of immersion time in the film formation was not described clearly.

Using the AAS result, the average daily dissolved ion of released ion of each material can be identified. This average daily dissolved ion is necessary to find the maximum ion released per day to compare with the maximum daily uptake level (Max UL). The maximum

TABLE 4. EDAX result of the oxide layer

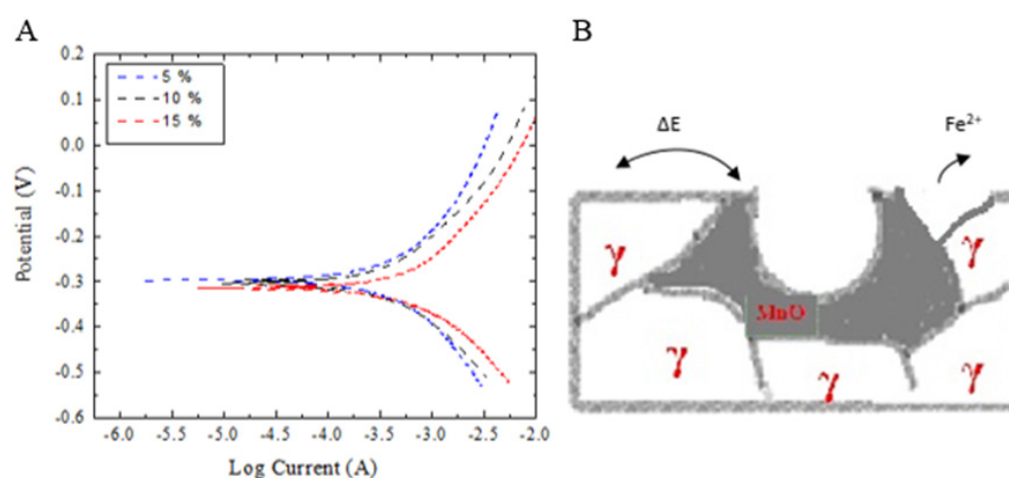| Element	wt. %	Analysis position
C	04.44	
O	30.58	
Cl	05.85	
Mn	09.22	
Fe	49.92	

FIGURE 5. (A) Potentiodynamic polarization diagram of Fe-Mn-C foam and (B) micro galvanic corrosion process illustration
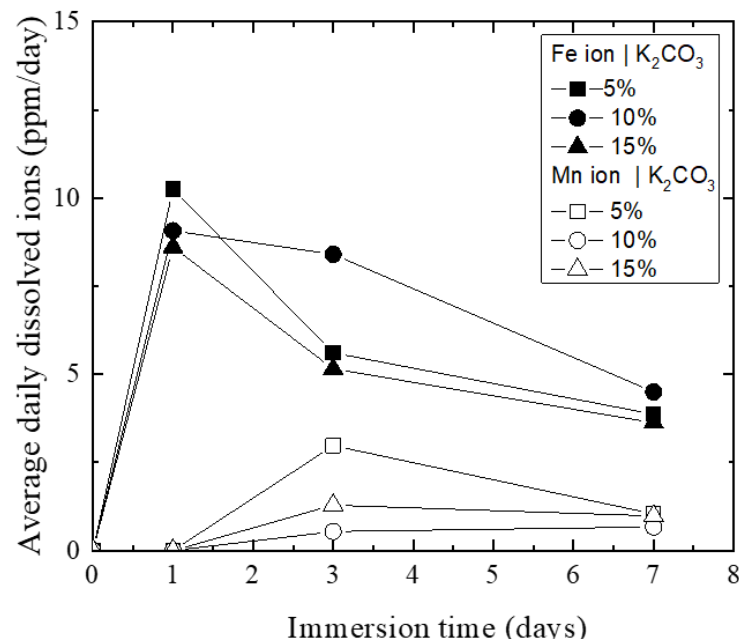
FIGURE 6. Daily dissolution of metals ion in the ringer solution

uptake level is the maximum allowable ion that can be tolerated by human bodies based on gender and age. To sum up, the ion concentration is still much lower than the maximum uptake level (UL) of manganese and iron for the human body. Manganese can be toxic if the concentration is above 11 mg/L, while the maximum iron concentration is 45 mg/L and the samples only release 10 ppm of iron and 2.5 ppm of manganese as the maximum number (Trumbo et al. 2001).

CONCLUSION

Porous structure of FeMnC alloys were successfully produced by powder metallurgy method with addition of K_2CO_3. The process succeeds in producing relatively low-density material dominated with austenitic phase. The density of the product reduced to 3.2 g/cm^3, about half of bulk material density, which are suitable for bone implant material. This study also showed that porosity affects the corrosion rate significantly due to the galvanic reaction between austenite and MnO. The galvanic reaction made higher iron ion release into the solution compared with manganese ion. At first 24 h, the ion released is dominated by the iron ion, and after 48 h our manganese started to release. However, a number of ion release from each element was below the daily uptake level for the human body.

REFERENCES

Benz, R., Elliott, J.F. & Chipman, J. 1973. Thermodynamics of the solid phases in the system Fe−Mn−C. *Metallurgical Transactions* 4(8): 1975-1986.

Čapek, J., Vojtěch, D. & Oborná, A. 2015. Microstructural and mechanical properties of biodegradable iron foam prepared by powder metallurgy. *Materials & Design* 83: 468-482.

Chakraborty Banerjee, P., Al-Saadi, S., Choudhary, L., Harandi, S.E. & Singh, R. 2019. Magnesium implants: Prospects and challenges. *Materials* 12(1): 136.

Feng, Y.P., Gaztelumendi, N., Fornell, J., Zhang, H.Y., Solsona, P., Baró, M.D. & Sort, J. 2017. Mechanical properties, corrosion performance and cell viability studies on newly developed porous Fe-Mn-Si-Pd alloys. *Journal of Alloys and Compounds* 724: 1046-1056.

Harjanto, S., Pratesa, Y., Suharno, B. & Syarif, J. 2012. Corrosion behavior of Fe-Mn-C Alloy as degradable materials candidate fabricated *via* powder metallurgy process. *Advanced Materials Research* 576: 386-389.

Huang, S.M., Nauman, E.A. & Stanciu, L.A. 2019. Investigation of porosity on mechanical properties, degradation and *in vitro* cytotoxicity limit of Fe30Mn using space holder technique. *Materials Science and Engineering: C* 99: 1048-1057.

Lehman, R.L., Gentry, J.S. & Glumac, N.G. 1998. Thermal stability of potassium carbonate near its melting point. *Thermochimica Acta* 316(1): 1-9.

Murphy, C.M., Haugh, M.G. & O'Brien, F.J. 2010. The effect of mean pore size on cell attachment, proliferation and migration in collagen-glycosaminoglycan scaffolds for bone tissue engineering. *Biomaterials* 31(3): 461-466.

Osorio-Hernández, J.O., Suarez, M.A., Goodall, R., Lara-Rodriguez, G.A., Alfonso, I. & Figueroa, I.A. 2014. Manufacturing of open-cell Mg foams by replication process and mechanical properties. *Materials and Design* 64: 136-141.

Pratesa, Y., Suharno, B., Wardhana, A.C. & Harjanto, S.J.J.T. 2019. Application of carbamide as foaming agent of Fe-

Mn-C alloy for degradable biomaterial candidate with powder metallurgy process. *Jurnal Teknologi* 81(1): 111-117 .

Pratesa, Y., Harjanto, S., Larasati, A., Suharno, B. & Ariati, M. 2018. Degradable and porous Fe-Mn-C alloy for biomaterials candidate. *AIP Conference Proceedings* 1933(1): 020007.

Šalak, A. & Selecká, M. 2012. *Manganese in Powder Metallurgy Steels*. Cambridge: Springer Science & Business Media. pp. 39-40.

Shah, F.A., Thomsen, P. & Palmquist, A. 2019. Osseointegration and current interpretations of the bone-implant interface. *Acta Biomaterialia* 84: 1-15.

Trumbo, P., Yates, A.A., Schlicker, S. & Poos, M. 2001. Dietary reference intakes: Vitamin A, vitamin K, arsenic, boron, chromium, copper, iodine, iron, manganese, molybdenum, nickel, silicon, vanadium, and zinc. *Journal of the Academy of Nutrition and Dietetics* 101(3): 294.

Witte, F., Hort, N., Vogt, C., Cohen, S., Kainer, K.U., Willumeit, R. & Feyerabend, F. 2008. Degradable biomaterials based on magnesium corrosion. *Current Opinion in Solid State and Materials Science* 12(5-6): 63-72.

Zhang, Q. & Cao, P. 2015. Degradable porous Fe-35wt.% Mn produced *via* powder sintering from NH_4HCO_3 porogen. *Materials Chemistry and Physics* 163: 394-401.

Yudha Pratesa & Sri Harjanto*
Research Center for Biomedical Engineering
Faculty of Engineering
Universitas Indonesia
Kota Depok, Jawa Barat 16424
Indonesia

Yudha Pratesa, Almira Larasati, Sri Harjanto*, Bambang Suharno & Myrna Ariati
Department of Metallurgical and Materials Engineering
Faculty of Engineering
Universitas Indonesia
Kota Depok, Jawa Barat 16424
Indonesia

*Corresponding author; email: sri.harjanto@ui.ac.id